ADVANCED FUNCTIONAL MATERIALS
www.afm-journal.de

Hydrogen-Bonded Organic Frameworks Enabling Highly Robust Aqueous Phase Ultralong Room-Temperature Phosphorescence

Wuzhen Luo, Jiayin Zhou, Yujing Nie, Feiming Li, Shunyou Cai, Guangqiang Yin, Tao Chen,* and Zhixiong Cai**

Aqueous phase room-temperature phosphorescence (RTP) materials are attracting increasing interest owing to their unique optical properties and promising applications. However, the realization of ultralong aqueous state RTP remains a formidable challenge due to severe quenching of triplet excitons in aqueous medium. In this study, a universal strategy is presented to achieve aqueous RTP materials through the encapsulation of organic phosphors within rigid hydrogen-bonded organic frameworks (HOFs) by in situ self-assembly. Benefiting from the compact and rigid microenvironments provided by HOFs, the nonradiative dissipations are immensely suppressed and populated triplet excitons are greatly stabilized by geometrical confinement and isolating organic phosphors from quenchers. As a result, the assembled HOFs-based materials reveal robust RTP emission with an ultralong phosphorescence lifetime of up to 493.1 ms and exhibit long-term optical and structural stability in water and even in harsh conditions (acid and base) for more than 10 days. Moreover, a fluorescent dye is introduced to finely tune the afterglow performance based on triplet-to-singlet Förster resonance energy transfer (TS-FRET), facilitating advanced information encryption and anticounterfeiting applications. This study provides a reliable and universal method to design and prepare robust RTP materials and expands their applications in advanced information encryption.

1. Introduction

Purely organic room-temperature phosphorescence (RTP) materials have gained increasing interest owing to their unique optical properties and promising applications in bioimaging, chemical sensing, information encryption, etc.[1] Compared with biological incompatibility and harsh preparation conditions of inorganic afterglow materials, organic RTP materials exhibit superior properties for their environmental friendliness, milder reaction conditions, and tunable optical performance. Over the past decades, several effective strategies such as crystal engineering,[2] covalent polymerization,[3] host–guest systems,[4] aggregation,[5] and doping in polymeric matrices[6] have been extensively established to achieve organic RTP materials. These successful approaches are primarily based on the promotion of the intersystem crossing (ISC) process by enhancing spin-orbit coupling (SOC) and the suppression of nonradiative dissipations by confining organic phosphors in rigid microenvironments.

In recent years, aqueous phase ultralong RTP materials have aroused intense attention for their great potential, particularly in bioimaging and water-based encryption ink.[7] In contrast to the extensive investigation of crystalline and amorphous polymer-based RTP, the aqueous phase RTP is still less explored and more challenging to be realized. Generally, the challenge to achieve RTP materials in water can be mainly attributed to the following two factors: i) the strong intermolecular interactions such as hydrogen bonding may be

W. Luo, Y. Nie, F. Li, S. Cai, Z. Cai
College of Chemistry
Chemical Engineering and Environment Fujian Provincial Key Laboratory of Modern Analytical Science and Separation Technology
Minnan Normal University
Zhangzhou, Fujian 363000, China
E-mail: czx1816@mnnu.edu.cn

J. Zhou, G. Yin, T. Chen
Country Ningbo Institute of Materials Technology and Engineering
Chinese Academy of Sciences
Ningbo, Zhejiang 315201, China
E-mail: yinguangqiang@nimte.ac.cn; tao.chen@nimte.ac.cn

The ORCID identification number(s) for the author(s) of this article can be found under https://doi.org/10.1002/adfm.202401728

F. Li, S. Cai, Z. Cai
Micro-Nano Organic Optical Materials Laboratory
Minnan Normal University
Zhangzhou, Fujian 363000, China

T. Chen
College of Material Chemistry and Chemical Engineering
Key Laboratory of Organosilicon Chemistry and Material Technology
Ministry of Education
Hangzhou Normal University
Hangzhou, Zhejiang 311121, China

DOI: 10.1002/adfm.202401728

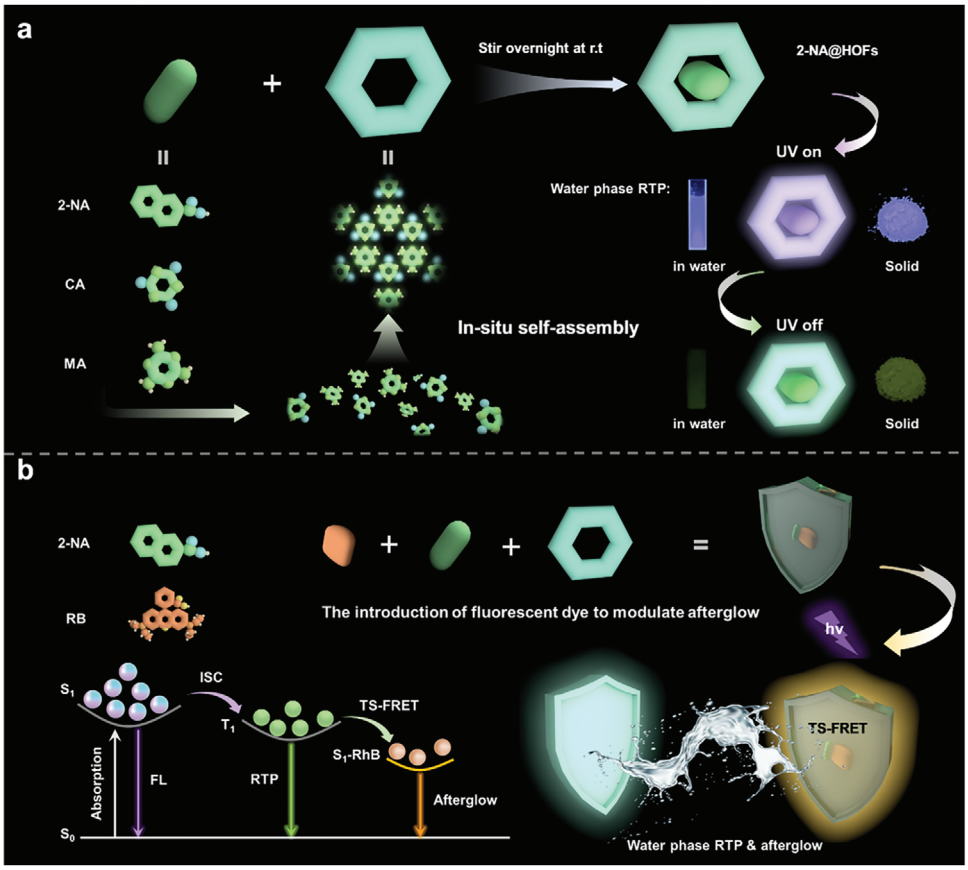

Scheme 1. The design and preparation strategy of robust RTP materials. a) Illustration of the preparation of ultralong robust RTP materials by encapsulating organic phosphors with HOFs. b) The regulation of afterglow performance based on TS-FRET.

interrupted and destroyed in water, leading to severe nonradiative dissipations from vigorous molecular motions; ii) the external quenchers such as dissolved oxygen can dramatically quench the populated triplet state excitons.[8] To address such knotty issues, several efficient methods have been established including the formation of organic nanoparticles,[9] macrocyclic supramolecular assembly,[10] in situ encapsulation within assembled hydrogen-bonded organic frameworks (HOFs),[11] and integrating phosphorescent molecules with supramolecular scaffolds.[12] Although these impressive strategies have significantly advanced the development of aqueous RTP materials, the corresponding phosphorescence lifetime is mostly in the microsecond range. Moreover, it lacks a universal strategy to access aqueous RTP materials without a tedious preparation process.

In this study, we present a universal and efficient strategy to obtain aqueous ultralong RTP materials with phosphorescence lifetimes of up to hundreds of milliseconds via an in situ assembly strategy (**Scheme 1**). To be specific, the RTP materials are efficiently prepared by in situ supramolecular assembly of melamine (MA), cyanuric acid (CA), and organic phosphors (Scheme 1a). It was reported that the MA-CA HOFs was insoluble and highly stable in water due to strong intermolecular interactions,[13] which makes it an excellent candidate for constructing robust RTP materials. Consequently, the phosphorescent molecules are well confined by the assembled HOFs to immensely inhibit nonradiative dissipations. Moreover, the robust and compact structure of HOFs provides an excellent quencher barrier for preventing organic phosphors from contacting dissolved oxygen and colliding with water molecules. As such, the resultant organic phosphors@HOFs show fantastic water resistance and maintain excellent RTP performance in the aqueous medium. To verify our hypothesis, naphthoic acid (NA) were first selected to construct RTP materials considering that aromatic carbonyl groups may enhance SOC to boost the ISC efficiency and the carboxylic acid groups can form strong hydrogen bonds with the HOF matrix to minimize the nonradiative dissipations. As anticipated, the prepared NA@HOF materials exhibit outstanding robust RTP performance in both solid state and aqueous medium. To further validate the universality, a series of phosphorescent molecules are rationally applied for constructing robust RTP materials, including biphenyldicarboxylic acid (BDA), terephthalic acid (TPA), 1-hydroxy-2-naphthalenecarboxylic acid (1-OH-2-NA), and 1-hydroxy-4-sulfamoyl-2-naphthalenecarboxylic acid (1-OH-4-SO_2NH_2-2-NA). In addition, a triplet-to-singlet Förster resonance energy transfer (TS-FRET)[14] platform is introduced for regulating afterglow performance by co-doping the acceptor dye Rhodamine B into the RTP system, leading to multicolor organic afterglow in both solid-state and aqueous medium (Scheme 1b). By leveraging these tunable water-based RTP inks,

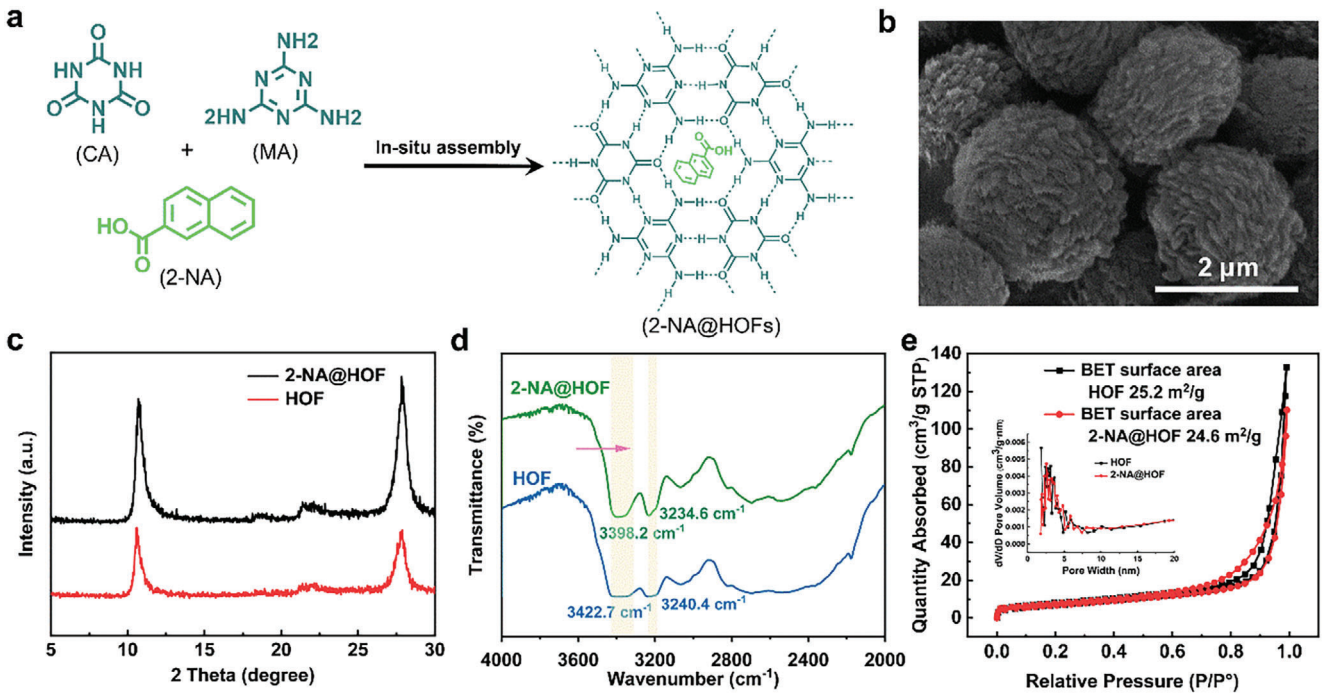

Figure 1. The characterization of in situ encapsulation of 2-NA. a) Schematic illustration for the formation mechanism of 2-NA@HOFs materials. b) SEM images of HOF. c) XRD of HOFs before and after 2-NA encapsulation. d) FT-IR spectra of HOF, 2-NA@HOFs. e) BET surface areas and Pore-size distribution of HOFs before and after the encapsulation of 2-NA.

high-level information encryption and anti-counterfeiting applications are successfully realized.

2. Results and Discussion

2.1. The Preparation and Characterization of NA@HOFs Materials

In this context, our goal is to develop a universal and reliable strategy to prepare robust aqueous phase RTP materials. For this purpose, 2-naphthoic acid (2-NA) was first applied for constructing robust RTP materials through in situ supramolecular self-assembly. The host-guest composite material, NA@HOFs, can be facilely prepared at room temperature via a facile in situ self-assembly approach MA, CA, and 2-NA (**Figure 1a**, see Supporting Information for experimental details). As shown in Figure 1b, scanning electron microscopy (SEM) images of the HOFs monomer confirm the plate-like structure of individual crystals, which are prone to aggregate into micrometer-sized particles. The morphology is further validated by transmission electron microscopy (TEM), exhibiting a clear visualization of the plate-like structure of individual crystals (Figure S1a, Supporting Information). The X-ray diffraction (XRD) pattern of NA@HOFs is consistent with blank HOFs (Figure 1c), indicating that the structural integrity of HOFs almost remains unchanged after the encapsulation of 2-NA molecules. Peaks observed at 10.7°, 18.5°, and 22.1° are attributed to the planar 2D hexameric structure of the HOF (Figure S1d, Supporting Information), while a characteristic peak at 27.8° indicates the presence of individual lamellar structures arranged in a graphite-like stacking manner. Additionally, SEM images of 2-NA@HOF indicate that the morphological features of the doped materials remain largely unchanged after encapsulating 1-NA or 2-NA molecules into the HOFs matrix (Figure S1b,c, Supporting Information). Furthermore, Fourier-transform infrared spectroscopy (FT-IR) confirms the successful preparation of the doped material (Figure 1d). The strong hydrogen bonding between 2-NA molecules and the HOFs matrix largely restricts the stretching motion of $-NH_2$, resulting in an obvious redshift of the $-NH_2$ stretching vibrations to lower frequencies. The peaks originally located at 3422.7 and 3240.4 cm^{-1} in HOFs monomer shift to 3398.2 and 3234.6 cm^{-1} after encapsulating 2-NA molecules. Lastly, N_2 adsorption/desorption isotherms provide further evidence of 2-NA encapsulation. Changes in the Brunauer–Emmett–Teller (BET) surface area and pore size before and after embedding 2-NA suggest the successful inclusion of guest molecules within the HOF framework (Figure 1e). These results comprehensively prove the structural integrity of HOFs the and successful encapsulation of 2-NA within the HOFs matrix.

To verify the impact of HOFs encapsulation on optical performance, we recorded the changes in the luminescence properties of the doped materials 2-NA by prompt and delayed emission spectroscopy. As depicted in **Figure 2a**, the prompt emission spectrum of 2-NA@HOFs displays an emission peak at 370 nm, while the delayed spectrum exhibits an emission peak at 527 nm. The average RTP lifetime at 527 nm was measured as 503.3 ms (Figure 2c), manifesting a long-lived feature. Notably, 2-NA@HOFs reveals a high quantum yield of up to 39.05% (Figure S3, Supporting Information). A visible green afterglow can be observed lasting for more than 2.0 s (Figure 2e, top). For

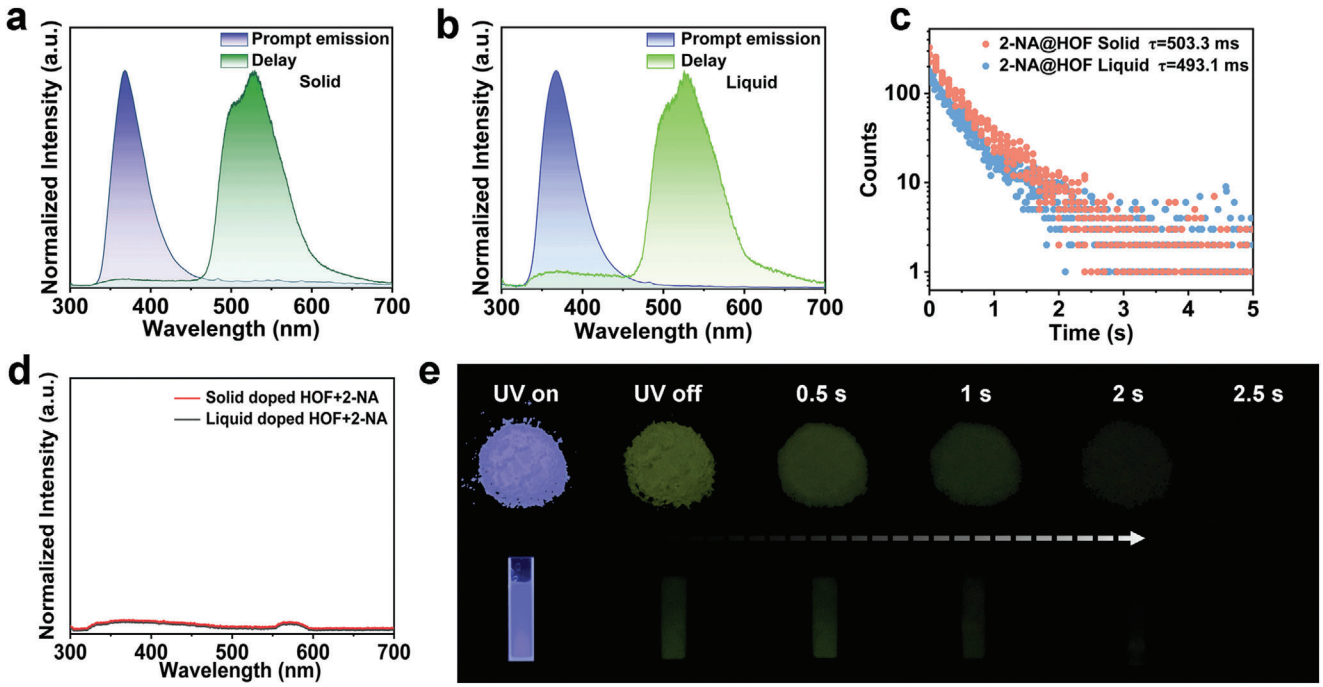

Figure 2. Optical properties of 2-NA@HOFs in both solid state and water. a) Prompt and delayed emission spectra of solid 2-NA@HOFs under ambient conditions. b) Prompt and delayed spectra of 2-NA@HOF aqueous dispersion. c) Phosphorescence lifetime decay profile of 2-NA@HOFs in solid state and aqueous medium. d) Phosphorescence emission spectra of mechanically ground HOFs+2-NA in solid state and aqueous medium. e) Photographs of luminescence of 2-NA@HOFs under a UV lamp and at different time intervals after the removal of UV irradiation.

comparison, we recorded the prompt and delayed emission spectra of 2-NA solid without encapsulation within HOFs (Figure S2, Supporting Information), where the prompt emission spectrum of 2-NA manifests an emission peak at 370 nm. However, green phosphorescent emission of 2-NA solid was not able to be observed. Furthermore, the phosphorescence decay profile signifies that millisecond-scale phosphorescence lifetime is absent. With no doubt, these results confirm that our in situ encapsulation strategy facilitates the stabilization of triplet excitons, leading to ultralong RTP emission with high quantum yield.

Remarkably, benefiting from the quencher barrier provided by rigid HOFs matrix, the doped material, 2-NA@HOF, maintains similar RTP performance to its solid-state counterpart in aqueous environments without any deoxygenation procedure (Figure 2b). The 2-NA@HOFs aqueous dispersion reveals a prompt emission peak at 370 nm and a delayed emission peak at 526 nm, with a phosphorescence lifetime of 493.1 ms (Figure 2c) and a quantum yield of 32.09% (Figure S3, Supporting Information). The aqueous dispersion displays a visible green afterglow with a duration of ≈2.0 s (Figure 2e, bottom). These results are in good agreement with its phosphorescent properties in the solid state, further suggesting that HOFs structure is robust and stable enough to immensely suppress the nonradiative dissipations and greatly stabilize the populated triplet excitons in aqueous medium. Therefore, 2-NA@HOFs can still maintain efficient RTP emission with phosphorescence lifetimes of up to hundreds of milliseconds in water. In order to exclude the influence of luminescence of blank HOFs (MA-CA), we further investigate the prompt and delayed emission properties of MA-CA HOFs (Figure S4, Supporting Information). The MA-CA HOFs shows a prompt emission at 368 nm in both the solid state and the aqueous medium. However, no visible RTP emission can be detected (Figures S4 and S5, Supporting Information). It demonstrates that the ultralong green RTP emission originates from the doped NA.

To further figure out the effect of the in situ encapsulation strategy on RTP emission, we prepared HOFs+2-NA doped material via a simple mechanical milling approach. As depicted in Figure 2d, no obvious delayed emission can be observed for resulting HOFs+2-NA doped material in both solid-state and aqueous medium. It suggests that mechanical milling alone cannot accomplish the encapsulation of organic phosphors for inhibiting the molecular motions and stabilizing the populated triplet excitons in the solid state, let alone in the aqueous medium. Overall, it can be concluded that encapsulation of organic phosphors in HOFs substrate by in situ supramolecular assembly strategy is crucial to achieve robust RTP materials in both solid state and aqueous phase. In addition, the influence of the doping ratio of guest molecule 2-NA on the luminescence properties was systematically investigated. It was found that the RTP performance had no significant variation by adjusting the fraction of dopant (Figure S6, Supporting Information). As depicted in Figure S6a,b (Supporting Information), the lifetimes were prolonged slightly at first and then shortened upon the increase of the doping ratio of 2-NA, indicating that a plethora of guest molecules was inadequate to be well encapsulated within the HOFs matrix. Accordingly, the afterglow emission follows the same trend with the lifetime (Figure S6c, Supporting Information). These subtle changes in the RTP performance further evidenced that 2-NA molecules can be efficiently and tightly immobilized within the rigid HOFs.

Likewise, the encapsulation of 1-naphthalenecarboxylic acid (1-NA) in the HOFs matrix exhibits satisfactory RTP performance. The 1-NA@HOFs composite material exhibits a prompt emission at 370 nm, and a phosphorescent emission peak emerges at 548 nm in the solid state (Figure S7a, Supporting Information). In addition, the phosphorescence lifetime of solid-state 1-NA@HOFs was measured as 255.1 ms (Figure S7d, Supporting Information), along with a decent quantum yield of 24.97% (Figure S8, Supporting Information, left). The mechanically ground composite materials fail to achieve long-lived RTP emission (Figure S7c,f, Supporting Information). Also, no visible RTP emission for 1-NA solid can be observed (Figure S9, Supporting Information). Owing to the protective environment provided by the HOFs matrix, 1-NA@HOFs in aqueous medium maintains a phosphorescence lifetime of 219.6 ms (Figure S7e, Supporting Information), accompanied by a quantum yield of 10.09% (Figure S8, Supporting Information, right). A yellow-green afterglow lasting for ≈1.0 s can be observed for both solid-state and aqueous-phase 1-NA@HOFs. Compared with 2-NA@HOFs, the performance degradation of 1-NA@HOFs may result from relatively weaker hydrogen bonding interactions between 1-NA molecules and HOFs matrix. Indeed, the theoretically calculated hydrogen bonding binding energy (ΔE_{HB}) of 1-NA@HOF and 2-NA@HOF are −75.217 and −78.385 kJ mol^{-1}, respectively (Table S1, Supporting Information). This result indicates that the hydrogen bonding interactions of 2-NA@HOF are stronger than that of 1-NA@HOF. Additionally, 1-NA@HOF displays a relatively smaller SOC value ($\xi(S_1, T_1)$ = 0.86 cm^{-1}) compared with 2-NA@HOF ($\xi(S_1, T_1)$ = 0.89 cm^{-1}), revealing a less ISC efficiency.

Additionally, long-term monitoring of NA@HOF aqueous dispersion demonstrates that their RTP performance is highly stable for more than 10 days (**Figure 3**a,b). For the sake of investigating the performance stability of the RTP materials in harsh conditions, we subjected the 1-NA@HOF and 2-NA@HOF to hydrochloric acid solution (pH = 2) and sodium hydroxide solution (pH = 12), respectively. Surprisingly, the emission of these two composite RTP materials displays almost the same peak positions and intensities in such a strong acidic and basic solutions compared with those in the water (Figure 3c,d). Accordingly, the fitting analyses of phosphorescence decay reveal that there is no significant change in lifetime (Figure 3e,f), indicating that the HOF has excellent acid and base resistance to maintain structural integrity. All these results manifest that the in situ assembled RTP materials are highly robust and maintain excellent optical performance in the water and even in harsh conditions.

To further elaborate on the ultralong RTP mechanism, we have undertaken an extensive investigation employing time-dependent density functional theory (TD-DFT) calculations by the Gaussian 16 program and PySOC program. It was found that the singlet-triplet splitting energy (ΔE_{ST}) has no obvious change before and after the encapsulation of NA within rigid HOFs matrix. To gain more insights into the high-performance RTP emission, we analyzed SOC constants, specifically from S_1 to T_n and from T_1 to S_0. Notably, the encapsulation of both 1-NA and 2-NA within HOF resulted in a substantial increase in SOC values. For 1-NA, efficient SOC channels include S_1-T_1 and S_1-T_3, with corresponding values of $\xi(S_1, T_1)$ = 0.09 cm^{-1} and $\xi(S_1, T_3)$ = 0.08 cm^{-1} (Figure S10a, Supporting Information). The SOC values were largely increased for 1-NA@HOF, specifically $\xi(S_1, T_1)$ = 0.86 cm^{-1} and $\xi(S_1, T_3)$ = 0.17 cm^{-1} (Figure S10b, Supporting Information). Similarly, the SOC values were slightly increased after the encapsulation of 2-NA within HOFs (Figure S10c,d, Supporting Information). According to the Franck–Condon principle, the rate of ISC is primarily determined by the singlet-triplet SOC and the energy gap (ΔE_{st}). Thus, it can be concluded that the enhanced SOC of NA@HOFs plays an important role in the promotion of the ISC process. The populated triplet excitons can be further well stabilized by compact and ordered microenvironments of HOFs, leading to long-lived RTP emission.

In addition, we analyzed a surface electrostatic site map to demonstrate the hydrogen bonding interactions between HOFs and NA molecules. The surface electrostatic potential analysis highlights the effective hydrogen donor and acceptor sites within MA, CA, and NA (Figure S11a, Supporting Information). This analysis underscores the in situ encapsulation between HOFs and NA through host-guest interactions, which contributes to the formation of NA@HOF. Moreover, the favorable hydrogen bonding environment established by HOF hosts plays a pivotal role in creating a rigid molecular framework to guarantee robust RTP emission of NA@HOF (Figure S11b,c, Supporting Information).

2.2. Proof of Universality and Regulation of RTP Performance

To prove the universality of the in situ assembly strategy and regulate RTP emission, we systematically introduced a series of compounds modified with aromatic carbonyl groups into the MA-CA HOF matrix to prepare robust RTP materials. Biphenyldicarboxylic acid (BDA), terephthalic acid (TPA), 1-hydroxy-2-naphthalenecarboxylic acid (1-OH-2-NA), and 1-hydroxy-4-sulfamoyl-2-naphthalenecarboxylic acid (1-OH-4-SO_2NH_2-2-NA) were rationally selected as guest molecules for being encapsulated into the HOF matrix. As shown in **Figure 4**a, BDA@HOF shows a blue–violet fluorescence emission at 358 nm, while displays green delayed emission is located at 526 nm with a phosphorescence lifetime of 324.3 ms in the solid state. As expected, BDA@HOF also exhibit excellent RTP performance in the water with a lifetime of up to 330.3 ms, which is not significantly different from that in the solid state. A green afterglow lasting for 1.5 s can be observed in both solid state and water after turning off 254 nm UV light (Figure 4b). Notably, the TPA@HOF exhibits intense deep blue fluorescence and RTP emission (Figure 4c), along with a long-lived lifetime of up to 435.2 and 441.5 ms in the solid state and aqueous medium, respectively. As such, the deep blue afterglow is visible for more than 3.5 s (Figure 4d). Similarly, 1-OH-2-NA@HOF and 1-OH-4-SO_2NH_2-2-NA@HOF also demonstrate the desirable RTP properties (Figure 4e–h). These results confirm the universality of the in situ assembly strategy for constructing robust RTP materials without tedious preparation procedures.

In addition to the aforementioned regulation, we employed an efficient TS-FRET strategy to modulate afterglow color to meet more application scenarios (**Figure 5**d). As a proof-of-concept, we utilized 2-NA as the energy donor and the commercially available fluorescent dye Rhodamine B (RB) as the energy acceptor to construct a TS-FRET platform. As depicted in Figure 5a, the UV absorption spectrum of RB overlaps well with the phosphorescence

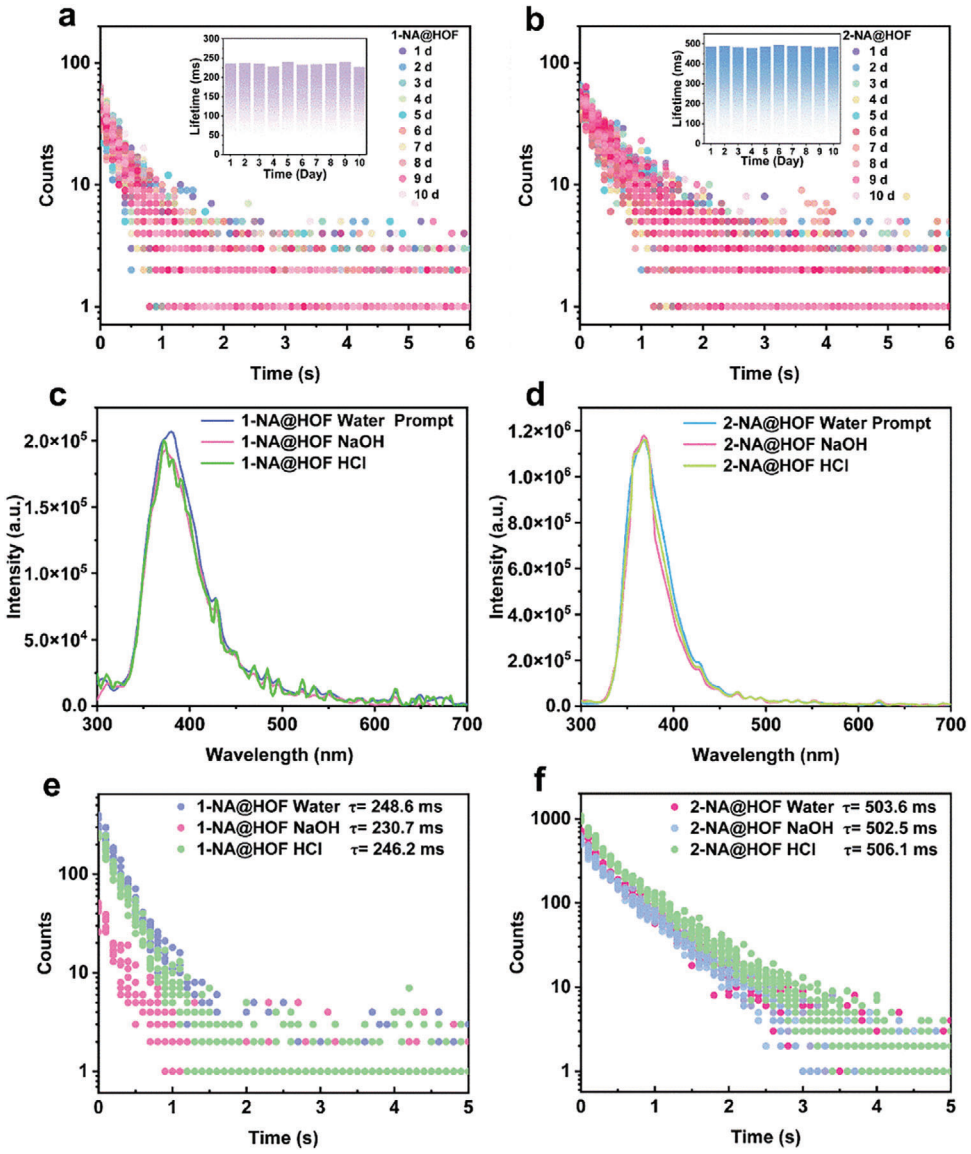

Figure 3. Validation of robust RTP emission in water and harsh conditions. a,b) 1–10 days phosphorescence lifetime decay spectrum of 1-NA@HOFs and 2-NA @HOFs in water. c,d) Prompt emission spectra of 1-NA@HOF and 2-NA@HOF in hydrochloric acid solution (pH = 2), sodium hydroxide solution (pH = 12), and water, respectively. e,f) Phosphorescence lifetime decay spectrum of 1-NA@HOF and 2-NA@HOF in hydrochloric acid solution (pH = 2), sodium hydroxide solution (pH = 12), and water, respectively.

emission spectrum of 2-NA@HOFs, satisfying the prerequisite for the TS-FRET process. It's found that the emission of the energy donor 2-NA gradually diminishes with increasing the doping concentration of RB, along with enhancing emission from the energy acceptor RhB (Figure 5b,c). To be specific, the doped material 2-NA+0.5RB@HOFs (2-NA/RB = 2:1) exhibits obvious RB emission at 578 nm under a 254 nm UV lamp, accompanied by a disappearance of RTP emission of 2-NA. By adjusting the doping concentration of RB, colorful afterglow from green to orange can be facilely realized. Remarkably, the afterglow regulation is not limited to the solid state but also can be realized in an aqueous medium (Figure 5e). For comparison, no RTP emission of the RB@HOFs material was observed, suggesting that the sustained luminescence of RhB originates from the TS-FRET process from the energy donor 2-NA. These results demonstrate that the afterglow performance can be efficiently regulated via TS-FRET, providing colorful afterglow emission in both solid state and aqueous conditions.

2.3. Information Encryption and Anti-Counterfeiting Applications

By taking advantage of these robust and tunable RTP materials, high-level spatial-time-resolved information encryption and anti-counterfeiting can be facilely realized. As a proof-of-concept, 2-NA@HOFs, 1-NA@HOFs, and their RB co-doped RTP materials were utilized for creating different patterns. As depicted in **Figure 6a** and Figure S14 (Supporting Information), we devised

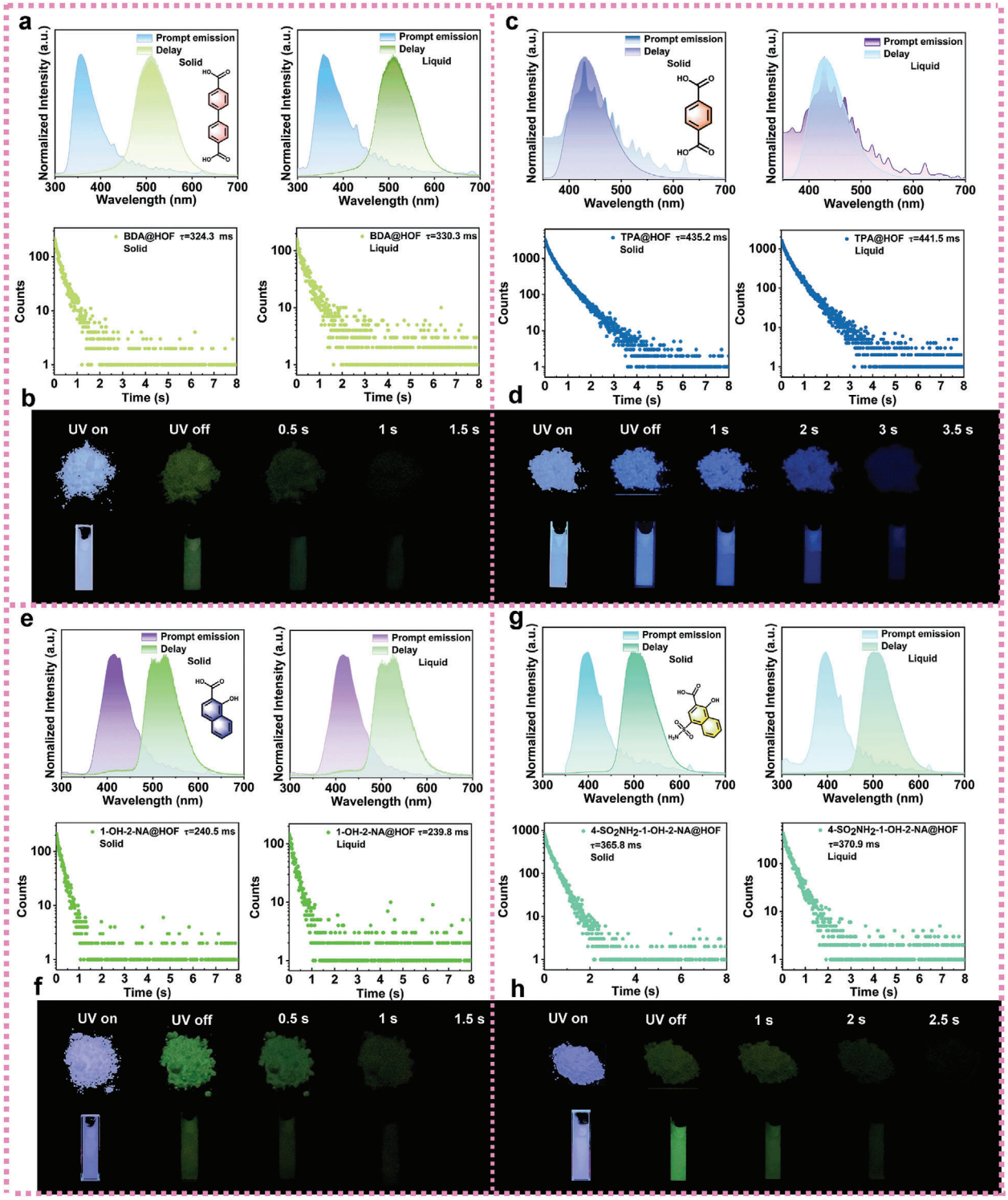

Figure 4. Proofing the universality of in situ assembly strategy to obtain robust HOFs-based RTP. a) Optical characterizations of BDA@HOFs. b) Photographs of BDA@HOFs under UV irradiation and at different time intervals after the removal of UV light. c) Optical characterizations of TPA@HOFs. d) Photographs of TPA@HOFs under UV irradiation and at different time intervals after the removal of UV light. e) Optical characterizations of 1-OH-2-NA@HOFs. f) Photographs of 1-OH-2-NA@HOFs under UV irradiation and at different time intervals after the removal of UV light. g) Optical characterizations of 1-OH-4-SO_2NH_2-2-NA@HOFs. h) Photographs of 1-OH-4-SO_2NH_2-2-NA@HOFs under UV irradiation and at different time intervals after the removal of UV light.

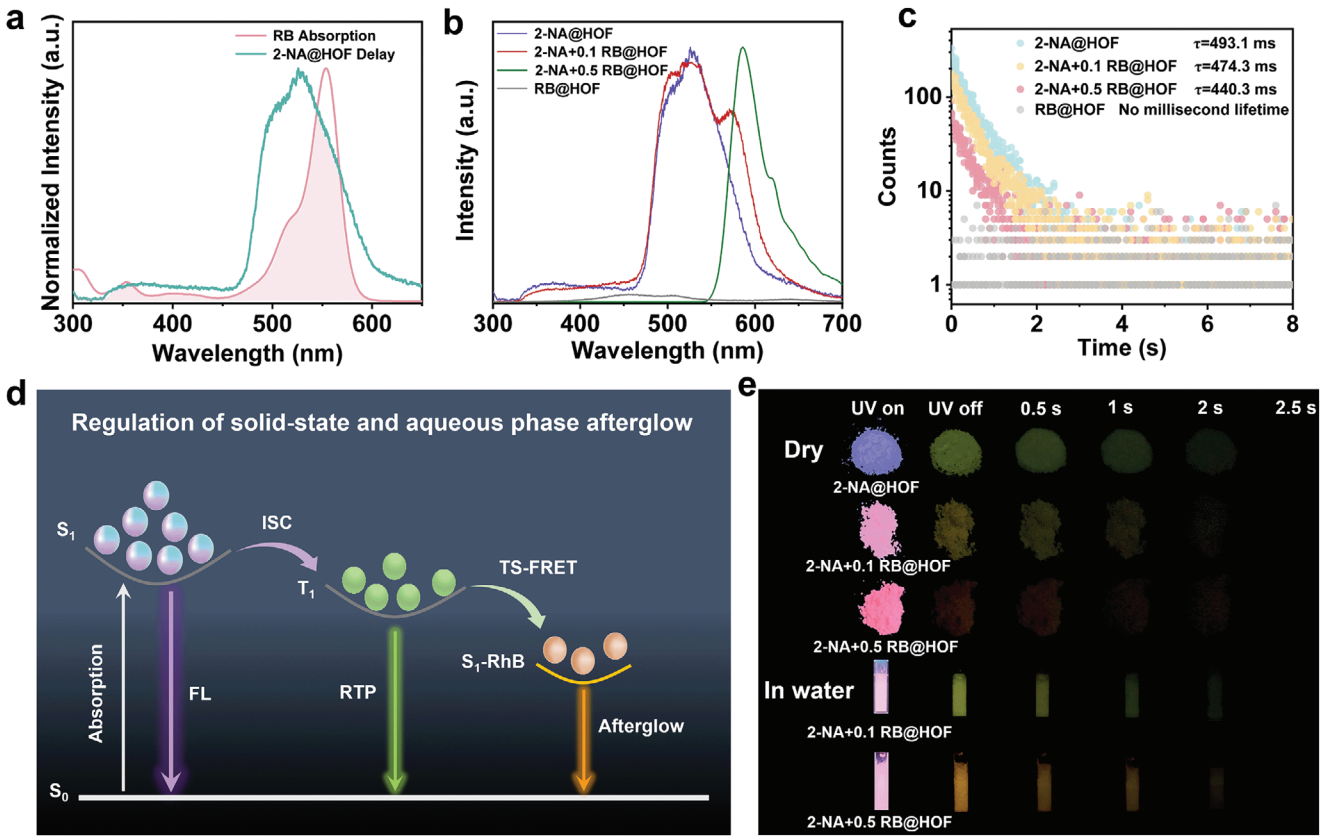

Figure 5. The regulation of afterglow emission by TS-FRET. a) UV–vis absorption spectrum of RhB, delayed emission spectrum of 2-NA@HOF, and prompt emission spectrum of RhB@HOFs in water. b) Delayed emission spectra of 2-NA@HOF, 2-NA+0.1 RhB@HOF, 2-NA+0.5 RhB@HOFs, RhB@HOFs RTP materials in water under 254 nm excitation. c) Phosphorescence lifetime decay profiles of composite RTP materials with different doping ratios of RhB in water. d) Simplified Jablonski diagram to illustrate the mechanism of TS-FRET. e) Photographs of luminescence of co-doped RTP materials with 2-NA+0.1 RB@HOFs, and 2-NA+0.5 RB@HOFs under 254 nm UV excitation and at different time intervals after the removal of UV light.

a "butterfly" pattern for the anti-counterfeiting icon with the border portion filled with blank solid HOFs powder. The upper half wings of the "butterfly" were filled with powder of 2-NA@HOFs doping material, while the lower half wings of the "butterfly" were filled with powder of 1-NA@HOFs. Under the illumination of a 254 nm UV lamp, a vivid "butterfly" pattern with intense blue–purple fluorescence appeared. Upon turning off the UV lamp, the luminescence of the border portion from HOF powder vanished rapidly, along with the appearance of a green "butterfly" pattern. Thereafter, the luminescence from the lower half of the wings of the "butterfly" composed of 1-NA@HOFs disappeared after turning off the UV lamp for 2 s, attributed to the shorter phosphorescent lifetime of 1-NA@HOFs. Such a dynamic evolution of the pattern showcases great potential for high-level spatial-time-resolved anti-counterfeiting applications.

More elaborate anti-counterfeiting patterns can be constructed as shown in Figure 6c,d. A logo representing "Minnan Normal University" was designed and created by using aqueous dispersions of HOFs-based materials (Figure 6c; Figure S16, Supporting Information). Such a characteristic logo was visible to the naked eyes under UV light. Upon deactivating the UV irradiation, the blue–purple luminescence from of borders, numerical sequence "1958" and the orange luminescence of the internal circular border faded out instantly, leaving the regions painted with long-lived RTP materials. Likewise, a vivid rose pattern was designed and painted by using HOF-based water-based inks (Figure 6d; Figure S17, Supporting Information). In addition to the vivid rose pattern under UV light, the pattern faded away in chronological order after the removal of UV irradiation. With no doubt, the security level of anti-counterfeiting is largely improved by the combination of HOFs-based RTP materials with different fluorescence emission and afterglow durations.

In addition to anti-counterfeiting applications, the HOFs-based RTP materials are highly desirable for information encryption (Figure 6b,e,f). First, we crafted the numerical sequence "8888" by selectively filling different segments with powders of 1-NA@HOF, 2-NA@HOF, RB@HOF, and 2-NA+0.5RB@HOF (Figure 6b; Figure S15, Supporting Information). Under the illumination of a 254 nm UV lamp, a segmented numerical display of "8888" emerged, with each segment emitting distinct colors. Upon turning off the UV lamp, the digits were transformed from "8888" to "8984" rapidly. Thereafter, the numerical sequence ultimately evolved into "3454" after turning off the UV light for 2.0 s. Similarly, a dot matrix was fabricated for information encryption, revealing dynamic evolution after turning UV light (Figure 6e; Figure S18, Supporting Information). More importantly, we designed a water-based collaborative encryption pattern by using 2-NA@HOF and 2-NA@PVA RTP

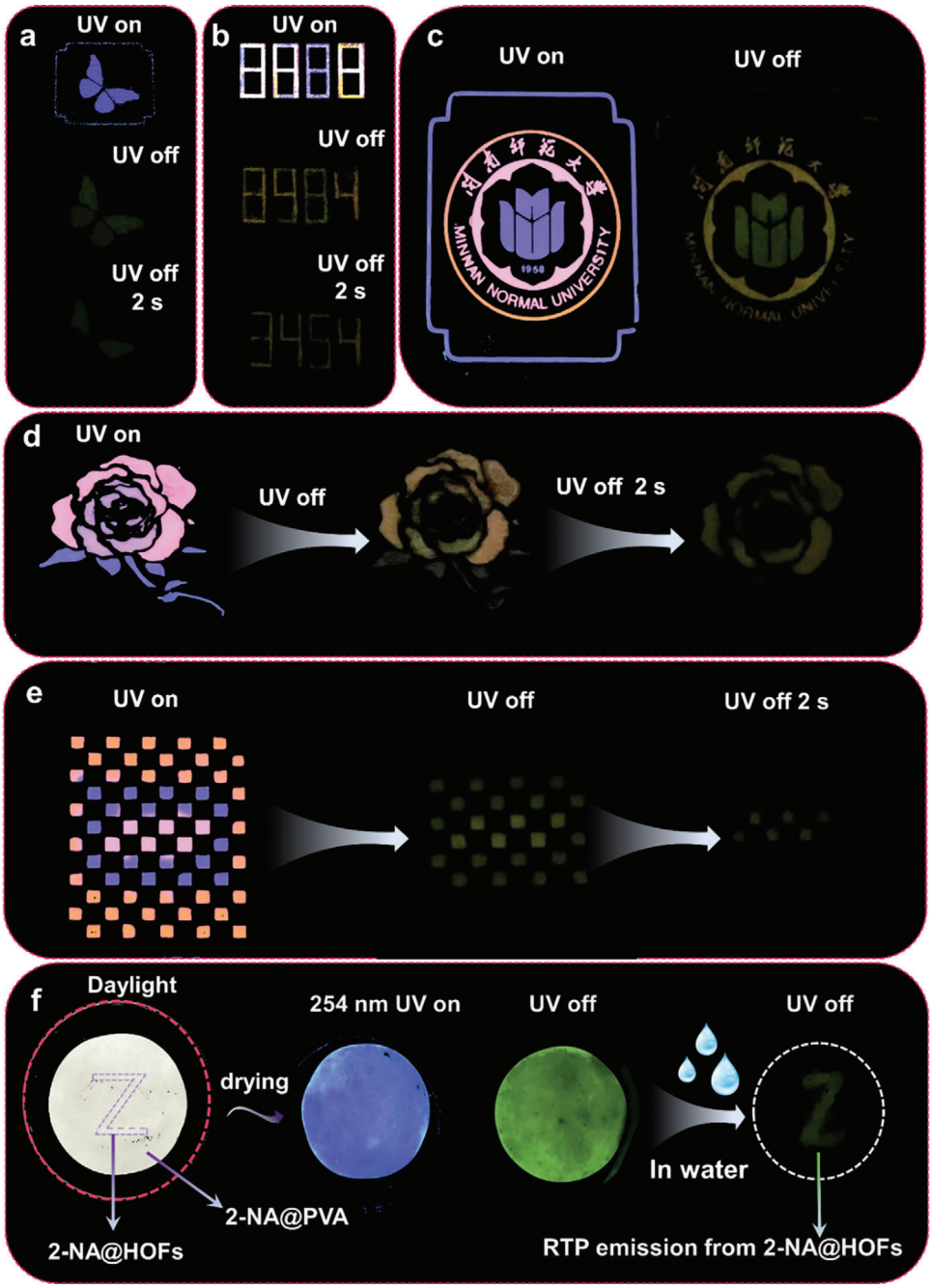

Figure 6. Applications of HOFs-based RTP materials in anti-counterfeiting and information encryption. a) The anti-counterfeiting butterfly pattern consists of HOFs (border), 1-NA@HOFs (lower half of the wings), and 2-NA@HOFs (upper half of the wings), respectively. b) Encryption pattern "8888" was prepared based on HOF-based RTP materials with different emission colors and lifetimes. c) The design and fabrication of the "Minnan Normal University" logo by the combination of HOFs-based RTP aqueous dispersions. d,e) Multicolored RTPs with "rose" and "checkerboard" patterns are composed of HOF-based RTP aqueous dispersions. f) Application of information encryption based on the different water-tolerance of 2-NA@PVA and 2-NA@HOFs RTP materials.

materials (Figure 6f). The 2-NA@PVA film was prepared by simply integrating 2-NA in the PVA matrix (see experimental details in Supporting Information), which exhibited excellent RTP emission (Figure S12, Supporting Information). However, the 2-NA@PVA film was extremely sensitive to water, resulting in RTP quenching (Figure S13, Supporting Information). Taking advantage of the different water tolerance, we impregnated filter paper with 2-NA@PVA material and subsequently wrote the letter "Z" using a 2-NA@HOF aqueous dispersion. After drying the filter paper, the target information "Z" was well hidden and couldn't be decrypted under daylight, UV light and instant cease of UV excitation. The only way to achieve target information is

by adding water based on the water-resistance of 2-NA@HOF and water-quenching of 2-NA@PVA. These preliminary results demonstrate that the HOF-based RTP materials are highly desirable for advanced anti-counterfeiting and information encryption applications with largely improved security level.

3. Conclusion

In summary, we have developed a universal and reliable approach to prepare robust RTP materials via in situ supramolecular self-assembly of HOFs. The rigid and compact microenvironments provided by the HOFs matrix not only immensely minimize the nonradiative dissipations but also provide quenching barriers for organic phosphors, leading to ultralong RTP emission in both solid state and aqueous medium. Significantly, the phosphorescence lifetime of the HOFs-based RTP materials reaches up to 493.1 ms, which is in sharp contrast to those reported materials with a lifetime in the microsecond level. Importantly, the in situ assembled HOFs-based RTP materials exhibit long-term stability, with no obvious optical performance degradation in water and harsh conditions (strong acidic and basic solution) for more than 10 days. Moreover, a series of molecules modified with aromatic carbonyl groups was introduced into the MA-CA HOFs matrix to validate the university of in situ supramolecular self-assembly strategy. As expected, all these HOFs-based RTP materials exhibit robust ultralong RTP emission in both solid state and aqueous medium. Besides, fluorescent dye RB was integrated into the HOFs-based RTP materials for modulating afterglow performance based on the TS-FRET mechanism. Consequently, the afterglow can be finely tuned from green to orange, providing colorful afterglow emission. Benefiting from their robust and tunable merits, these HOFs-based ultralong RTP materials are highly suitable for advanced anti-counterfeiting and information encryption applications. We believe that our strategy will pave a new avenue for realizing high-performance RTP in aqueous and harsh conditions.

Supporting Information

Supporting Information is available from the Wiley Online Library or from the author.

Acknowledgements

W.L. and J.Z. contributed equally to this work. The authors are grateful to the financial support from the National Natural Science Foundation of China (Grant 21904055 and 22205249), the Natural Science Foundation of Fujian province (Grant 2023J011815 and 2020J05164), Zhejiang Provincial Natural Science Foundation of China (LQ23B040002), and the Office of the President, Minnan Normal University (KJ18001).

Conflict of Interest

The authors declare no conflict of interest.

Data Availability Statement

The data that support the findings of this study are available from the corresponding author upon reasonable request.

Keywords

aqueous phosphorescence, encryption applications, hydrogen-bonded organic frameworks, robust, ultralong lifetime

Received: January 29, 2024
Revised: March 1, 2024
Published online:

[1] a) W. Zhao, Z. He, B. Z. Tang, *Nat. Rev. Mater.* **2020**, *5*, 869; b) S. Xu, R. Chen, C. Zheng, W. Huang, *Adv. Mater.* **2016**, *28*, 9920; c) T. Zhang, X. Ma, H. Wu, L. Zhu, Y. Zhao, H. Tian, *Angew. Chem., Int. Ed.* **2020**, *59*, 11206; d) Q. Liao, Q. Li, Z. Li, *Adv. Mater.* **2023**, 2306617. e) X. K. Ma, Y. Liu, *Acc. Chem. Res.* **2021**, *54*, 3403.

[2] a) H. Zhu, I. Badía-Domínguez, B. Shi, Q. Li, P. Wei, H. Xing, M. C. Ruiz Delgado, F. Huang, *J. Am. Chem. Soc.* **2021**, *143*, 2164; b) W. Li, Q. Huang, Z. Mao, X. He, D. Ma, J. Zhao, J. W. Y. Lam, Y. Zhang, B. Z. Tang, Z. Chi, *Nat. Commun.* **2022**, *13*, 7423; c) S. Garain, S. N. Ansari, A. A. Kongasseri, B. Chandra Garain, S. K. Pati, S. J. George, *Chem. Sci.* **2022**, *13*, 10011; d) S. Cai, H. Shi, Z. Zhang, X. Wang, H. Ma, N. Gan, Q. Wu, Z. Cheng, K. Ling, M. Gu, C. Ma, L. Gu, Z. An, W. Huang, *Angew. Chem., Int. Ed.* **2018**, *57*, 4005.

[3] a) L. Gu, H. Wu, H. Ma, W. Ye, W. Jia, H. Wang, H. Chen, N. Zhang, D. Wang, C. Qian, Z. An, W. Huang, Y. Zhao, *Nat. Commun.* **2020**, *11*, 944; b) X. Ma, C. Xu, J. Wang, H. Tian, *Angew. Chem., Int. Ed.* **2018**, *57*, 10854; c) H. Peng, G. Xie, Y. Cao, L. Zhang, X. Yan, X. Zhang, S. Miao, Y. Tao, H. Li, C. Zheng, W. Huang, R. Chen, *Sci. Adv.* **2022**, *8*, eabk2925; d) H. Gao, X. Ma, *Aggregate.* **2021**, *2*, e38.

[4] a) X. Ma, J. Wang, H. Tian, *Acc. Chem. Res.* **2019**, *52*, 738; b) J. Han, W. Feng, D. Y. Muleta, C. N. Bridgmohan, Y. Dang, G. Xie, H. Zhang, X. Zhou, W. Li, L. Wang, D. Liu, Y. Dang, T. Wang, W. Hu, *Adv. Funct. Mater.* **2019**, *29*, 1902503; c) Y. Wang, J. Yang, M. Fang, Y. Yu, B. Zou, L. Wang, Y. Tian, J. Cheng, B. Z. Tang, Z. Li, *Matter.* **2020**, *3*, 449; d) H. Sun, L. Zhu, *Aggregate.* **2023**, *4*, e253.

[5] a) Y. Zhang, Y. Su, H. Wu, Z. Wang, C. Wang, Y. Zheng, X. Zheng, L. Gao, Q. Zhou, Y. Yang, X. Chen, C. Yang, Y. Zhao, *J. Am. Chem. Soc.* **2021**, *143*, 13675; b) G. Jiang, J. Yu, J. Wang, B. Z. Tang, *Aggregate.* **2022**, *3*, e285; c) Q. Li, Z. Li, *Acc. Chem. Res.* **2020**, *53*, 962; d) J. Yang, M. Fang, Z. Li, *Aggregate.* **2020**, *1*, 6; e) G. Yin, W. Lu, J. Huang, R. Li, D. Liu, L. Li, R. Zhou, G. Huo, T. Chen, *Aggregate.* **2023**, *4*, e344; f) G. Yin, G. Huo, M. Qi, D. Liu, L. Li, J. Zhou, X. Le, Y. Wang, T. Chen, *Adv. Funct. Mater.* **2023**, 2310043.

[6] a) Y. Su, S. Z. F. Phua, Y. Li, X. Zhou, D. Jana, G. Liu, W. Q. Lim, W. K. Ong, C. Yang, Y. Zhao, *Sci. Adv.* **2018**, *4*, eaas9732; b) L. Ma, S. Sun, B. Ding, X. Ma, H. Tian, *Adv. Funct. Mater.* **2021**, *31*, 2010659; c) R. Tian, S. M. Xu, Q. Xu, C. Lu, *Sci. Adv.* **2020**, *6*, eaaz6107.

[7] a) H. Sun, L. Zhu, *Aggregate.* **2022**, *4*, e253. b) G. Yin, J. Zhou, W. Lu, L. Li, D. Liu, M. Qi, B. Z. Tang, P. Théato, T. Chen, *Adv. Mater.* **2024**, 2311347.

[8] a) Y. Liang, P. Hu, H. Zhang, Q. Yang, H. Wei, R. Chen, J. Yu, C. Liu, Y. Wang, S. Luo, G. Shi, Z. Chi, B. Xu, *Angew. Chem., Int. Ed.* **2024**, *63*, 202318516. b) J.-A. Li, L. Zhang, C. Wu, Z. Huang, S. Li, H. Zhang, Q. Yang, Z. Mao, S. Luo, C. Liu, G. Shi, B. Xu, *Angew. Chem., Int. Ed.* **2023**, *62*, 202217284.

[9] a) M. Palner, K. Pu, S. Shao, J. Rao, *Angew. Chem., Int. Ed.* **2015**, *54*, 11477; b) X.-F. Wang, H. Xiao, P.-Z. Chen, Q.-Z. Yang, B. Chen, C.-H. Tung, Y.-Z. Chen, L.-Z. Wu, *J. Am. Chem. Soc.* **2019**, *141*, 5045; c) X. Zhen, Y. Tao, Z. An, P. Chen, C. Xu, R. Chen, W. Huang, K. Pu, *Adv. Mater.* **2017**, *29*, 1606665; d) Q. Dang, Y. Jiang, J. Wang, J. Wang, Q. Zhang, M. Zhang, S. Luo, Y. Xie, K. Pu, Q. Li, Z. Li, *Adv. Mater.* **2020**, *32*, 2006752; e) X. Jia, C. Shao, X. Bai, Q. Zhou, B. Wu, L. Wang, B. Yue, H. Zhu, L. Zhu, *Proc. Natl. Acad. Sci.* **2019**, *116*, 4816; f) T. Weng, Q.

Zou, M. Zhang, B. Wu, G. V. Baryshnikov, S. Shen, X. Chen, H. Ågren, X. Jia, L. Zhu, *J. Phys. Chem. Lett.* **2021**, *12*, 6182; g) S. Cai, H. Shi, J. Li, L. Gu, Y. Ni, Z. Cheng, S. Wang, W.-w. Xiong, L. Li, Z. An, W. Huang, *Adv. Mater.* **2017**, *29*, 1701244.

[10] a) D. Li, Z. Liu, M. Fang, J. Yang, B. Z. Tang, Z. Li, *ACS Nano.* **2023**, *17*, 12895; b) J. Wang, Z. Huang, X. Ma, H. Tian, *Angew. Chem., Int. Ed.* **2020**, *59*, 9928; c) W.-L. Zhou, Y. Chen, Q. Yu, H. Zhang, Z.-X. Liu, X.-Y. Dai, J.-J. Li, Y. Liu, *Nat. Commun.* **2020**, *11*, 4655; d) X.-Y. Dai, M. Huo, X. Dong, Y.-Y. Hu, Y. Liu, *Adv. Mater.* **2022**, *34*, 2203534.

[11] Q.-Q. Xia, J.-L. Yu, Z.-Y. Chen, Z.-Y. Xue, X.-H. Wang, X. Liu, M.-X. Wu, *Cell Rep. Phys. Sci.* **2023**, *4*, 101494.

[12] a) S. Kuila, K. V. Rao, S. Garain, P. K. Samanta, S. Das, S. K. Pati, M. Eswaramoorthy, S. J. George, *Angew. Chem., Int. Ed.* **2018**, *57*, 17115; b) X. Yao, J. Wang, D. Jiao, Z. Huang, O. Mhirsi, F. Lossada, L. Chen, B. Haehnle, A. J. C. Kuehne, X. Ma, H. Tian, A. Walther, *Adv. Mater.* **2021**, *33*, 2005973; c) L. Zhu, M. T. Trinh, L. Yin, Z. Zhang, *Chem. Sci.* **2016**, *7*, 2058; d) J. Liu, Y. Sun, G. Wang, X. Chen, J. Li, X. Wang, Y. Zou, B. Wang, K. Zhang, *Adv. Opt. Mater.* **2022**, *10*, 2201502.

[13] V. R. Pedireddi, D. Belhekar, *Tetrahedron.* **2002**, *58*, 2937.

[14] a) X. Wang, G. Pan, H. Ren, J. Li, B. Xu, W. Tian, *Angew. Chem., Int. Ed.* **2022**, *61*, 202114264; b) Y. Zhao, L. Ma, Z. Huang, J. Zhang, I. Willner, X. Ma, H. Tian, *Adv. Opt. Mater.* **2022**, *10*, 2102701.